Charge Trapping in Amptek CdTe Detectors

Amptek's XR-100-CdTe detectors are high performance X-ray detectors, ideal for X-ray spectroscopy above 25 keV. The efficiency of a 0.75 or 1 mm CdTe detector is very high even at the U K_α X-ray line, 98 keV, while the energy resolution is close to the Fano limit above 25 keV. For these reasons, CdTe detectors are commonly used at energies above 25 keV.

But CdTe detectors differ from Si detectors in a few important details. Many of these differences are discussed elsewhere, in another Amptek application note and in a recent research paper. One important difference is in the important of charge trapping, leading to hole tailing. This note provides background information on the origin and consequences of trapping. An understanding of trapping is important to permit users and system designers to obtain the best performance for their particular applications. This note begins with a brief review of the general properties of semiconductor nuclear detectors for users who are new to this field. The note then discusses the properties of CdTe that affect operational performance, particularly charge trapping. Finally, this note discusses the characteristics of Amptek's XR-100-CdTe systems and their use in various applications.

Charge trapping effects appear in many compound semiconductors used in radiation spectroscopy. This application note focuses on Amptek products, which currently use CdTe (a special case of $Cd_{1-x}Zn_xTe$), but the equations and the general results of this note apply to any planar detectors in which charge trapping is important, i.e., HgI_2, PbI_2, etc.

1 INTRODUCTION

1.1 REVIEW OF THE PROPERTIES OF SEMICONDUCTOR NUCLEAR DETECTORS

All radiation detection is based on the fact that ionizing radiation, by its very definition, generates free electrons and ions (or holes) in the medium in which it interacts. The charge generated is proportional to the energy deposited: when an energy E_0 is deposited, it will produce a $N_0=E_0/\varepsilon_{pair}$ carriers. In a semiconductor, the energy per electron-hole pair is roughly 3.4 times the bandgap. Under an applied electric field these electrons and holes will drift towards their respective oppositely charged electrodes, as sketched in Figure 1. The motion of the carriers from the point of interaction to the contact generates a transient current I(t) in the detector, and by current continuity into the electronics.

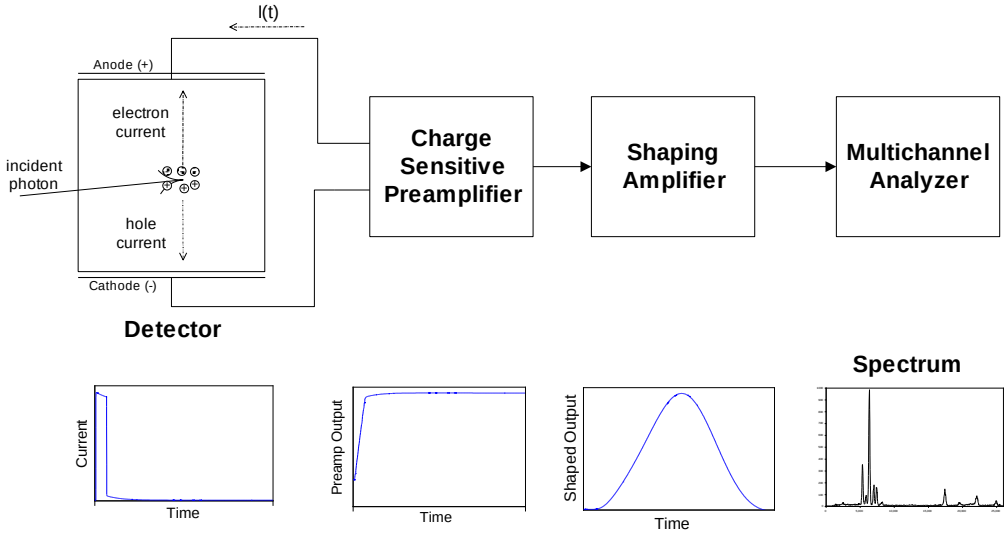

Figure 1. Schematic diagram of the detector and electronics. Typical outputs from each stage of the processing electronics are sketched below.

In most applications, one is interested in measuring the deposited energy, which is proportional to the total charge rather than the current. Charge is the integral of current so the detector is attached to a charge-sensitive preamplifier, which produces an output pulse with a voltage step directly proportional to the time integral of the current. The preamp output is then sent to a shaping amplifier, which shapes the pulse to

allow accurate measurements under realistic conditions, amplifies them, and filters out noise to maximize the signal-to-noise ratio. The shaped and amplified pulse, a voltage pulse with peak amplitude proportional to the deposited energy, is then sent to a multichannel analyzer, which measures the peak amplitude of many pulses, producing a histogram showing the number of pulses with amplitude measured within the range of each channel. This is the output spectrum.

In an ideal detector, every X-ray or γ-ray photon of a given energy incident on the detector would interact and produce a voltage pulse of exactly the same amplitude. For a monoenergetic source, all of the counts would be in a single channel and the count rate would equal the rate of incident photons. This is not the case in practice. A typical real spectrum, showing the characteristic X-rays emitted by lead and measured by an XR-100T-CdTe, is shown in Figure 2.

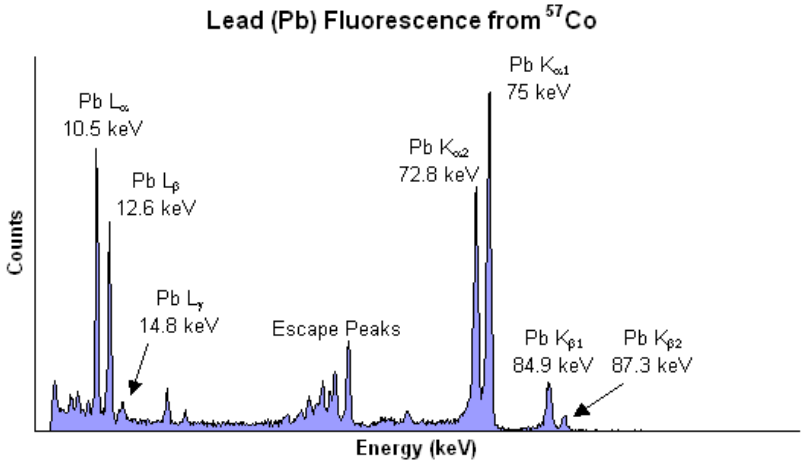

Figure 2. Representative spectrum from Pb X-Rays measured using an Amptek XR-100T-CdTe system. The finite peak widths and the background continuum and peaks are clearly seen.

A real detector deviates from the ideal for many reasons. Some photons do not interact at all, but pass through the detector. Some of the photons which interact will scatter from the detector or produce secondary emissions within the detector, depositing only a portion of the incident energy. The result is a rather complicated response function, which depends on the properties of the incident radiation and on the material and size of the detector. For those events depositing full energy, various processes lead to a finite width for the peak, the energy resolution. These processes include statistical fluctuations in charge generation, trapping of carriers leading to fluctuations in the transient current, and electronic noise. The most important electronic noise sources are current and voltage fluctuations into the preamplifier input, caused by shot noise in the leakage current through the detector and thermal noise in the preamplifier input circuitry.[i]

1.2 Compound Semiconductors in Nuclear Detection

In general, one would like a detector with very high sensitivity, in which the maximum number of particles interact and contribute to the full-energy peak, and with very high energy resolution, to separate closely spaced peaks and to quickly identify peaks above the background. In practice, there is a trade-off to be made between sensitivity and resolution. Practical matters, such as size, ruggedness, or the need for cryogenic cooling make further trade-offs necessary. The best energy resolution for X-rays and γ-rays is obtained using Si or Ge diode detectors, if they are cryogenically cooled to reduce leakage currents and thermal noise. The primary disadvantage of Si and Ge detectors is the need for cryogenic cooling. There are many applications where cooling the detector with liquid nitrogen is impractical, due to constant replenishment or due to the physical size and weight of the cryostat.

The best sensitivity for γ-rays is obtained using scintillators, such as NaI(Tl). Scintillators are crystals in which the energy deposited produces optical photons, which are then detected by a photodetector, which produces the transient current input to the electronics. The crystals can be fabricated in very large volumes (tens of centimeters), and the light transported over large distances, resulting in excellent sensitivity. However, the resolution is limited by the fact that very few photons are detected and by the nonlinearity in

the scintillator's response. Photomultiplier tubes can detect the photons with high performance, but these tubes are physically large and mechanically fragile and have low sensitivity. Photodiodes can also be used but the electronic noise of the diodes further degrades the energy resolution.

A variety of applications require better resolution than can be achieved with scintillators but where cryogenic cooling is not practical. The ideal detector for such applications would have a bandgap much larger than that of Si or Ge, since leakage current at a given temperature decreases exponentially with the bandgap. The ideal detector would also have a high atomic number and density, because the photoelectric cross-section increases as Z^5 and the attenuation is proportional to density. This permits a much smaller detector volume for equal stopping power.[ii] Several semiconductors meet these criteria. Unlike Si and Ge, these high-Z wide bandgap semiconductors are all compound semiconductors, made of two or more elements. The compound semiconductors most commonly used in nuclear detection applications are CdTe, its cousin $Cd_{1-x}Zn_xTe$ (CZT), and HgI_2. Many other compound semiconductors have been studied and have found some uses, including CdSe, PbI_2, TlBr, $TlBr_{1-x}I_x$, InP, and others[iii].

Although these compound semiconductors have certain advantages over Si and Ge, including higher attenuation coefficients and (in principal) lower bulk leakage currents due to the wider bandgap, they also have some significant disadvantages. The primary disadvantage is that they have a far higher density of defects in the crystal lattice, resulting in a large number of trapping sites, leading to carrier transport properties far inferior to those of Si and Ge. Because of this, practical detector sizes are quite limited and even within the limited size, considerable spectroscopic distortion is observed. Further, leakage currents are often dominated by the defects so are not as low as might be expected from the bandgap. Other disadvantages are related to uniformity and stability of the material.

In spite of these disadvantages, compound semiconductors are the best solution for a wide variety of applications. To obtain the best performance, the user should recognize the disadvantages and how to address them. This is discussed in detail below. This section concentrates on CdTe, but the results are generally applicable to all of the wide-bandgap, high-Z semiconductors.

2 CHARGE TRANSPORT

Consider again the charge transport and signal generation process sketched in Figure 1. At the electric field strengths usually found in a radiation detector, the drift velocity v of the carriers is proportional to the electric field strength $\mathcal{E}$, where the constant of proportionality is defined as the mobility μ, $v=\mu\mathcal{E}$. The instantaneous current is I=qnv, where q is the charge on an electron, n is the number of carriers, and v is their mean velocity. The duration of the transient current pulse is determined by the distance the carriers must travel. There will clearly be two distinct current pulses, one from holes and one from electrons, where the electrons will produce a much higher current for a shorter time, due to their higher mobility.

The simplest case is that of a uniform, planar detector of thickness L with a bias *V*, giving a constant and uniform electric field, $\mathcal{E}=V/L$. Consider an X-ray which deposits energy E_0 at a depth x. The interaction generates charge Q_0, which gives rise to electron and hole currents I_e and I_h, which flow for a duration of T_e and T_h. In the absence of trapping, these quantities will be given by

$$Q_0 = qN_0 = q\left(\frac{E_0}{\varepsilon_{pair}}\right) \qquad I_{h0} = Q_0\left(\frac{\mu_h\mathcal{E}}{L}\right) \qquad I_{e0} = Q_0\left(\frac{\mu_e\mathcal{E}}{L}\right) \qquad T_e = \frac{L-x}{\mu_e\mathcal{E}} \qquad T_h = \frac{x}{\mu_h\mathcal{E}}$$

The induced charge, the time integral of the current which is measured by the preamp, will be independent of depth:

$$Q = \int I(t)dt = I_{e0}T_e + I_{h0}T_h = Q_0\left(\frac{\mu_e\mathcal{E}}{L}\right)\left(\frac{L-x}{\mu_e\mathcal{E}}\right) + Q_0\left(\frac{\mu_h\mathcal{E}}{L}\right)\left(\frac{x}{\mu_h\mathcal{E}}\right) = Q_0$$

The size of the voltage step at the preamplifier output is $V=Q/C_F$, where C_F is the preamplifier feedback capacitance. For the XR-100T, C_F is about 50 fF.

These equations apply to all planar devices with a uniform field, regardless of the material. Analogous equations can be derived for other geometries. The numerical values depend upon the material so will be

different for CdTe and CZT. In fact, there can be some difference from one detector to another due to manufacturing differences. Typical values for 1 mm XR-100T-CdTe, 0.75 mm –CdTe, and the older -CZT are given in the table below. The top rows are typical material properties, while the middle rows show typical values for detectors available from Amptek. Note that the nominal thickness is different for the two detectors. The last rows show quantities for a 59.5 keV X-ray which interacts in the middle of the detector.

	CdTe		CZT
Material Properties			
ε_{pair} (eV)	4.43	4.43	5.0
μ_e (cm^2/V-sec)	1100	1100	1350
μ_h (cm^2/V-sec)	100	100	120
τ_e (μsec)	3	3	1
τ_h (μsec)	2	2	0.05
Detector Properties			
L (cm)	0.1	0.075	0.2
V (volts)	400	500	400
Interaction Properties			
N_0 (electron-hole pairs)	$1.3x10^4$	$1.3x10^4$	$1.2x10^4$
Q_0 (Coulomb)	$2.1x10^{-15}$	$2.1x10^{-15}$	$1.9x10^{-15}$
I_e (nA)	95	210	26
I_h (nA)	8.6	19	2.3
T_e center (nsec)	12	5	37
T_h center (nsec)	125	56	415
T_e max (nsec)	23	10	74
T_h max (nsec)	250	112	830

2.1 TRAPPING

Whenever excess charge is generated in a semiconductor, thermal equilibrium is disturbed. The semiconductor returns to equilibrium via recombination, which occurs at trapping sites[iv]. The number of free charges decays exponentially, with lifetimes τ_e and τ_h for the electrons and holes respectively. In Si and Ge, there are few trapping sites and the carrier lifetimes are several milliseconds long. A negligible fraction of the charges will be trapped during the charge collection process. For the compound semiconductors used in radiation detection, modern crystal growth practices lead to a much higher density of defects, which are trapping sites, and hence shorter lifetimes. For CZT, typical lifetimes might be $\tau_e=1x10^{-6}$ sec and $\tau_h=0.05x10^{-6}$ sec. Because the hole lifetime is much shorter than the hole transit time, the induced current is significantly reduced, and further, it depends upon the depth of interaction in the detector. The time integral of the current induced into the preamplifier is called the induced charge. Figure 3 below is a plot comparing currents and induced charge for an interaction 0.25 mm into a 2 mm thick CZT detector. It should be noted that there exists a very wide variation in the hole lifetime from one detector to the next. This is not well controlled by current manufacturing practices and can easily vary over an order of magnitude.

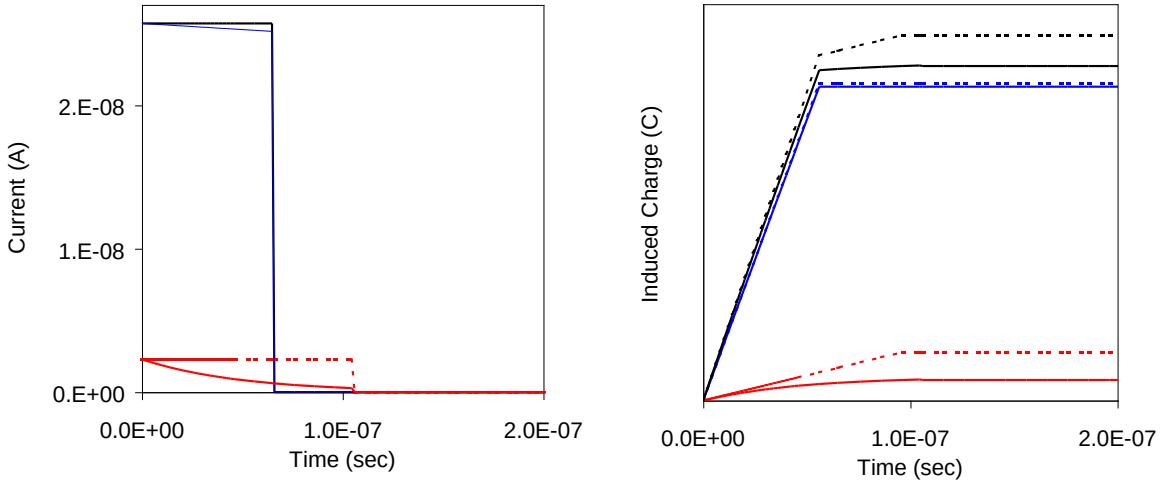

Figure 3. Computed transient currents and induced charge. Left: computed transient current for an interaction at 0.25 mm in CZT. Electron currents are shown in blue, hole currents in red. The dashed lines indicate the values expected in the absence of trapping, while the solid lines indicate the values expected for a real detector. Right: computed preamplifier output, for the same case.

For CdTe, the hole lifetime is typically 2×10^{-6} sec, more than an order of magnitude larger than in CZT. The hole lifetime is comparable to or greater than the hole transit time, so the charge deficit is much smaller. The charge loss is not negligible but is much smaller than in CZT, under identical conditions. This is a primary reason for the use of the CdTe detectors. Furthermore, the new CdTe detectors have a diode structure, which allows a higher bias voltage to be applied with little increase in electronic noise. Since the transit time goes down with bias, this reduces the charge loss even further. And the CdTe diodes are thinner, further increasing the electric field and also decreasing the distance the charges must travel. The result is a dramatic enhancement in the quality of the spectrum.

Quantitatively, the charge collection efficiency η is defined as the total induced charge divided by the charge created, Q/Q_0. It is a function of depth and is generally written in terms of the trapping length, $\lambda_e=(\mu_e\tau_e)\mathcal{E}$ and similarly for λ_h. For a uniform internal electric field, it is given by the Hecht relation[v]:

$$\eta(x) = \frac{\lambda_e}{L}\left(1 - e^{-\frac{x}{\lambda_e}}\right) + \frac{\lambda_h}{L}\left(1 - e^{-\frac{L-x}{\lambda_h}}\right)$$

For the Amptek XR-100T-CZT with the 50 nsec hole lifetime, λ_e=2.7 cm while λ_h=0.01 cm. The electrons are nearly all collected, but clearly the holes will not be fully collected. Figure 4 is a plot showing the charge collection efficiency versus depth. For interactions near the front contact, virtually all charge is collected, because the trapping time for the electrons is long compared with the transit time. For interactions near the rear contact, the induced charge is very small. Note, however, that it is non-zero. The tailing does not extend to zero amplitude. For the XR-100-CdTe, which is 1 mm thick, λ_e=13.2 cm while λ_h=0.8 cm. A much larger fraction of the hole signal is collected.

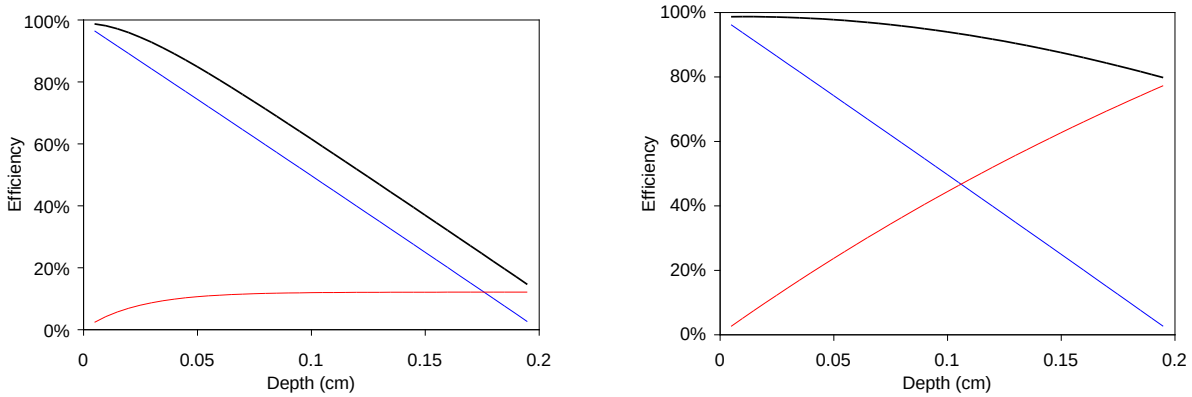

Figure 4. Plot of computed charge collection efficiency versus depth for an Amptek XR-100T-CZT(left) and -CdTe (right) with a 1 mm thick element. For the CZT, photons interacting deep inside the detector will clearly produce a much smaller signal than those interacting near the front contact. The effect is much smaller for the CdTe.

2.2 CONSEQUENCES FOR RADIATION SPECTROSCOPY

The result of trapping for spectroscopy is an effect known as "hole tailing." Consider the case where the attenuation length is long relative to detector thickness, so there is equal probability of interaction at each point in the detector. From Figure 4 above, about one-eighth of the interactions will occur near the front contact, in the region of the detector where charge collection efficiency (CCE) is maximum and constant. Interactions occurring deeper will create a smaller signal, with the smallest signals arising from interactions at the cathode, where the signal is entirely due to the hole current. Since the plots curve down, successively smaller signals are generated over smaller volumes and hence have fewer counts. Qualitatively, the result is a "tail" sloping down from the energy of the peak to a minimum at the CCE of the cathode. The consequence for spectroscopy is that, instead of a simple Gaussian with a small tail extending smoothly to zero, a significant fraction of the counts occur in the tail and the tail terminates at a specific value. To accurately determine net area, the tail must be included as part of the photopeak.

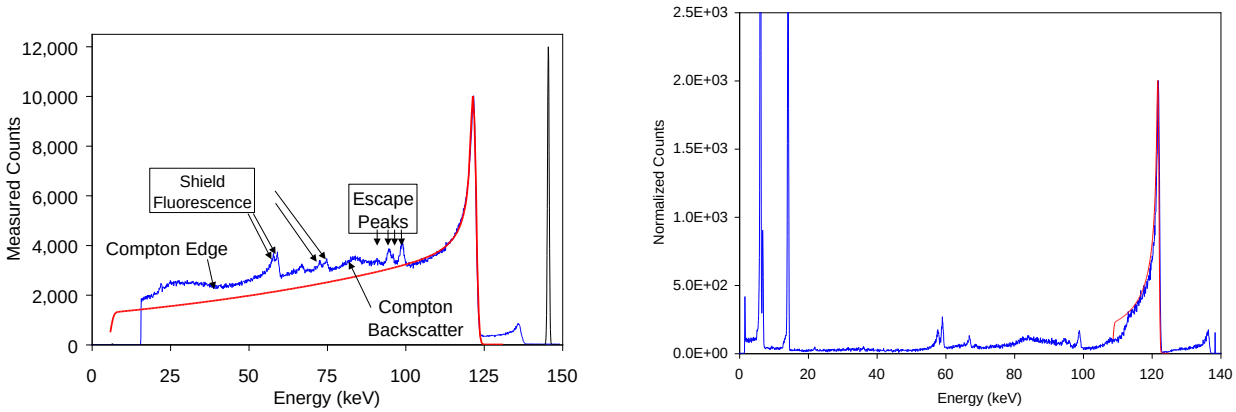

Figure 5. Computed and measured spectra obtained from ^{57}Co with an XR-100T-CZT detector (left) and a 1 mm -CdTe detector (right).

Given these qualitative results, many users raise a series of questions, which will be answered in the section below:

- How can I model the photopeak shape in my spectral analysis software?

- What is the quantitative shape of the photopeak? What does it depend on?
- How does the shape vary with energy?
- How does the shape vary with applied voltage?
- How reproducible is the shape from one detector to the next?
- How stable is the shape over time?

2.3 QUANTITATIVE MODEL OF PHOTOPEAK SHAPE

2.3.1 Peak Modeling for Spectral Analysis

A quantitative model for the photopeak shape is very important for spectral analysis. It is useful for determining net area and critical for finding overlapping peaks. Amptek has developed an accurate, "physics-based" model, described below. Unfortunately, it is not in a closed form: there is no simple equation for this model. It is useful for understanding the phenomena of hole tailing and for predicting system performance during design, but it is not helpful for fitting spectra.

The photopeak shape for Si and Ge detectors is usually modeled as the sum of three terms: a noise Gaussian, a step function, and then an exponential tail, which extends smoothly and continuously down. The CdTe tail is different since it drops to zero below the charge collection efficiency of the cathode. The simplest way to model the CdTe spectra is to use the Gaussian and exponential terms of the Si fit but to terminate them at the cathode CCE: modify the exponential by adding a step function. The plot below shows results for the 122 keV peak of ^{57}Co.

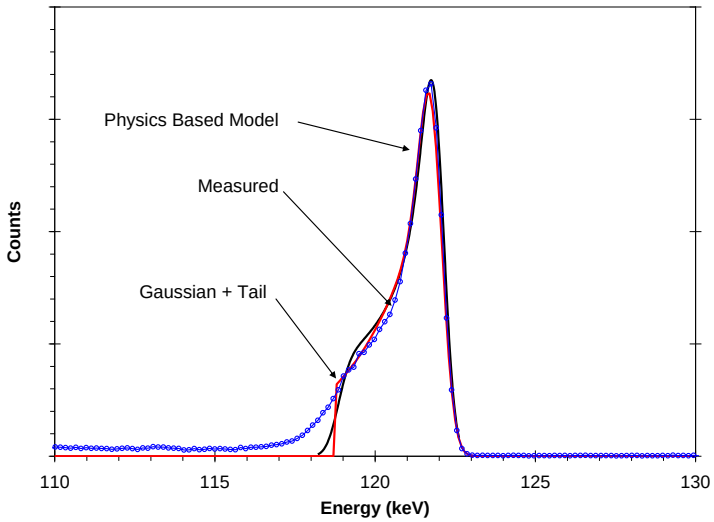

Figure 6. Plot comparing a measured 122 keV photopeak (blue), the results of the "physics-based" model (black), and an empirical fit using a Gaussian and a terminated exponential (red).

The step in the tail will, for any particular detector, be a constant fraction of the photopeak energy (97.4% in this case). The width of the Gaussian includes three terms: the noise (constant), Fano broadening (scales as $\sqrt{E}$) and an empirical term reflecting the combination of these with the tail. The fraction of counts in the tail will vary with energy.

2.3.2 Physics-Based Model

Amptek has developed a "physics-based" model, which is useful to understand hole tailing and to predict how the photopeak shape will vary with bias voltage, energy, temperature, or any other parameter. The model incorporates three effects: radiation interactions, charge collection, and electronic noise.

For low energies, the radiation interaction is modeled as purely photoelectric attenuation, which gives the probability of interaction at any depth as P(x). Figure 7 shows, in blue, the fraction of photons interacting (per unit length) in each depth of the detector, for 122 keV incident photons. The red curve shows η(x), the charge collection efficiency, versus depth, using the Hecht equation above for a uniform electric field. The pulse height is η(x). The spectrum is the probability P of measuring a pulse height Q so, if we had no noise, it would be given by the combination of these curves, P(x(Q)). This requires inverting the Hecht equation and since there is no closed form, this is done numerically. The black curve on the right of Figure 7 shows P(Q), the noiseless pulse height spectrum due to hole tailing. To model noise, the hole tailing spectrum is convolved with a Gaussian function, which includes electronic noise and Fano broadening. This yields the blue curve shown on the right of Figure 7.

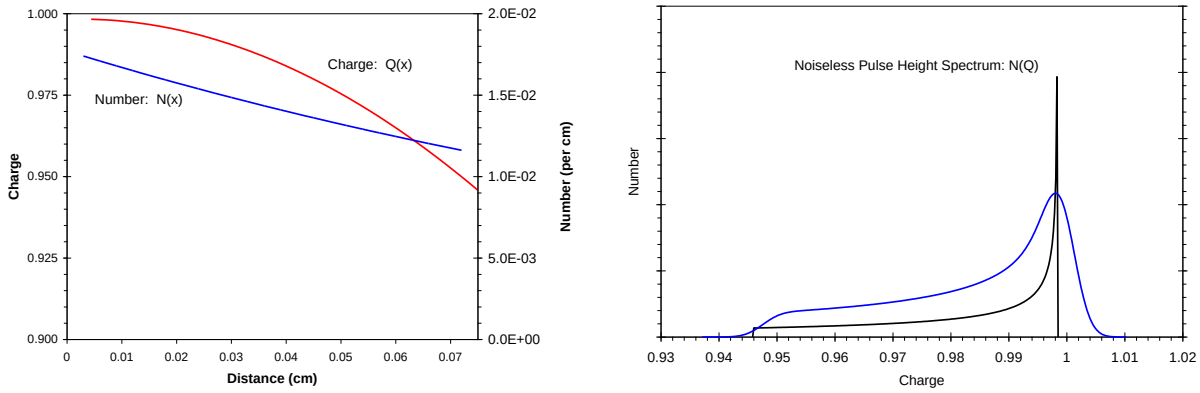

Figure 7. Plots illustrating the photopeak shape model.

Figure 6 compares a model spectrum (in black) with data (in blue) for a 0.75 mm CdTe detector at 500V, measuring 122 keV photons. There is a very close match, differing only at the low energy end of the tail, which terminates more sharply in the model. This probably arises from the non-uniform field in the diode: holes traveling the full distance experience a weak-field region, so the charge loss is greater than expected from a uniform, mean-field.

At higher energies, the capture of Compton secondaries becomes important. Events near the peak (tail) correspond to the full energy of the event being deposited near the cathode (anode). If a photon Compton scatters at one point, and then the Compton secondary is absorbed in the detector, then the full energy is deposited, but not at a single point. It is highly unlikely that both interactions will occur near either contact; even if one interaction occurs at a contact, the other will likely occur nearer the middle. Therefore, we intuitively expect an enhancement of counts with charge collection "in the middle."

This was quantitatively modeled using the ACCEPT Monte Carlo software package. The detector volume was divided into 50 μm slices, and for each incident photon, the energy deposited in each slice was computed. The effective charge from each slice was computed using the Hecht equation. The results are shown in Figure 8. Even though the hole tailing terminates at the same fractional charge collection, the full width at half maximum of the peak is much larger when capture of Compton secondaries is important. At 662 keV, 66% of the full energy deposition events (in a 1 mm detector) involve Compton scatter followed by photoelectric absorption of the secondary photon.

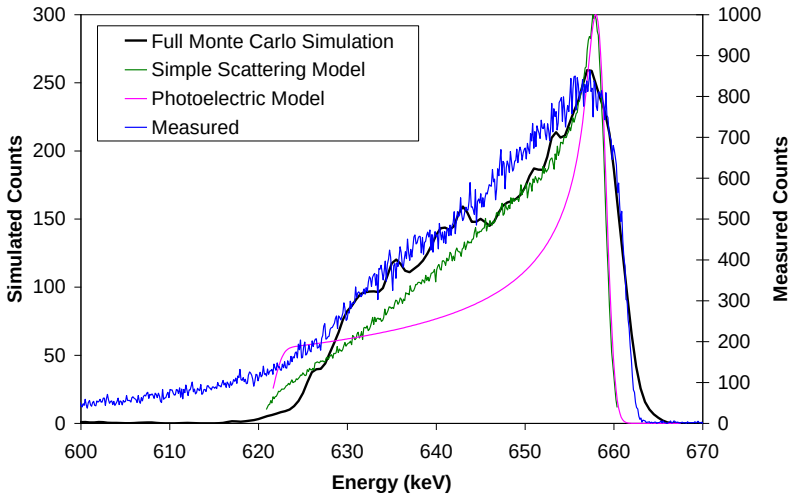

Figure 8. Photopeak spectrum observed with a 1 mm CdTe detector at 662 keV. The blue curve represents the observed spectral shape. The pink curve shows the result of a simple model, neglecting Compton scattering and including photoelectric absorption, charge transport, and electronic noise. The green curve is a very simple model for the capture of Compton secondaries. The black curve is the result of the full Monte Carlo simulation[i].

2.3.3 Variation with Energy

Figure 9 and Figure 10 show how the peak shape varies with energy. These spectra were measured with a 5x5x0.75 mm^3 CdTe diode at 500V and 230K. The charge collection at the anode is 98%, independent of energy. At the lowest energy, the peak is nearly Gaussian: virtually all of the interactions occur where charge collection efficiency is 100%. In Figure 10, the blue dots show the data, the black curve the model result, and the red curve a simple Gaussian. At the 59.5 and 88 keV peaks, the asymmetry is visible but looks like a small tail on a Gaussian. At 122 keV, however, the distinct tail is visible, along with its termination.

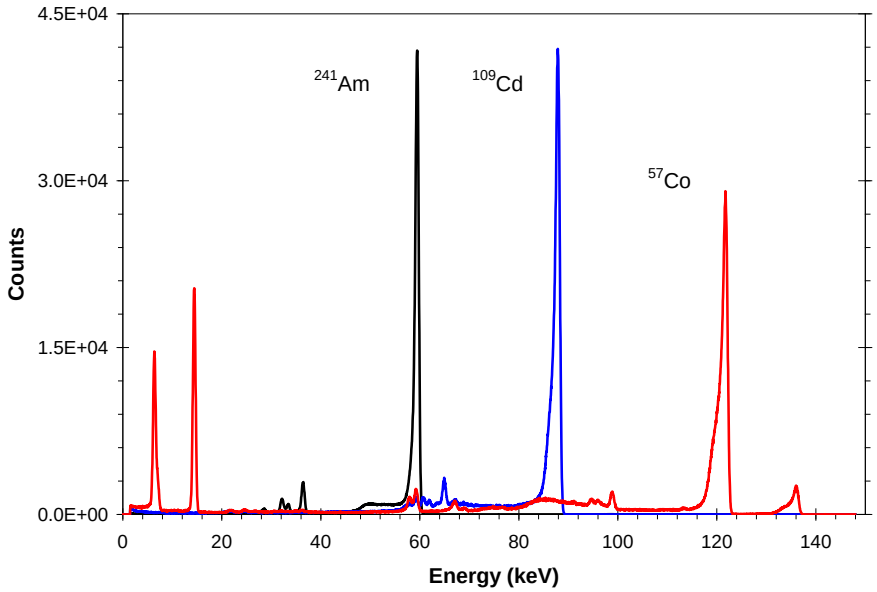

Figure 9. Spectra showing the variation of the peak shape with energy, below 150 keV.

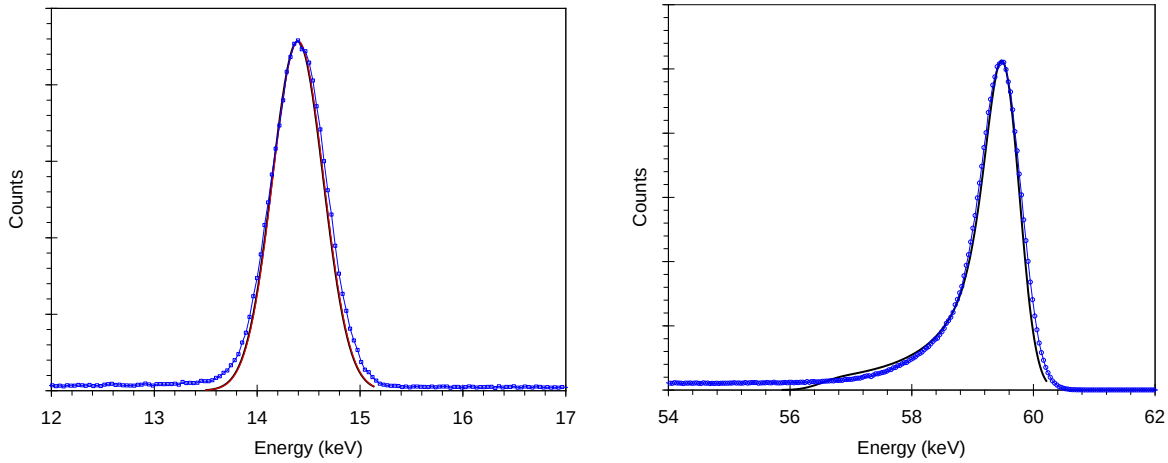

Figure 10. Plots showing measured and modeled photopeak spectra. The left shows the 14.4 keV photopeak from ^{57}Co while the right shows the 59.5 keV peak from ^{241}Am.

2.3.4 Variation with Bias Voltage

As bias voltage is increased two things occur: charge collection improves but electronic noise degrades. At low energies, the resolution is dominated by electronic noise, so resolution will get worse with increasing bias voltage. At high energies, resolution is dominated by charge collection, so will improve with increasing bias voltage. Figure 11 shows the clear improvement in photopeak shape seen at 122 keV as bias voltage is raised to 750V. The net area of the three peaks is the same, but at lower bias more counts are in the tail.

For the 14.4 keV peak in these three measurements, the best resolution and highest peak amplitude were found in the 250V spectrum. The optimum bias for a particular application depends on the energy of primary interest.

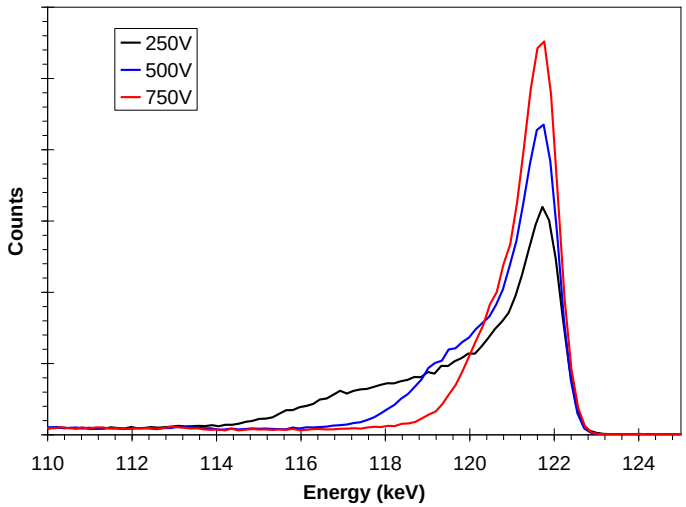

Figure 11. Three ^{57}Co spectra measured with a 0.75 mm CdTE detector at bias voltages of 250, 500, and 750V.

3 OTHER CHARACTERISTICS

3.1 UNIFORMITY

The existing state-of-the-art of crystal growth produces considerable macroscopic non-uniformity in the crystals of compound semiconductors. A single boule will often contain several crystalline regions, with different orientations and obviously a high density of crystal defects along the boundary. If a radiation detector is cut from a region containing two crystals, there will be many defects and hence a short lifetime. Moreover, the conductivity is usually larger along a grain boundary, which alters the applied electric field. In a polycrystalline detector, the electric field will not be uniform and constant. There are other macroscopic defects which can alter the charge collection properties. For example, it is possible for Te inclusions to form. This leads to a small metallic region, which obviously alters the internal electric field.

Even in the absence of macroscopic defects, it is common to observe variations in the material properties over the volume of a detector. For example, the Cd to Zn ratio can vary radially in the grown crystal, due to thermal gradients. This causes the bandgap to vary over the volume of a detector, and hence the charge per pair, causing an obvious peak broadening. Spatial variations in the trap density cause spatial variations in the lifetime and hence in the tailing. One region of the detector might produce much worse tailing than another.

The result of a non-uniform electric field or non-uniform trapping lifetimes will be to alter the detailed shape of the hole tailing. The general properties of the tail will remain, but the detailed shape will not match that given by the Hecht equation and shown in Figure 5.

3.2 STABILITY

The stability of a spectrum over time is very important for quantitative analysis. Unfortunately, there exists considerable confusion in the literature regarding the stability of CdTe and polarization. Details are given below, but the key points to note aRe (1) CdTe Schottky diodes do exhibit polarization, but (2) polarization is important at room temperatures and low bias voltages, so (3) under the operating conditions of Amptek's XR100-CdTe and stack, polarization is not important.

As sketched in Figure 12, when a radiation interaction occurs, the electrons and holes travel towards the contacts. In the presence of trapping sites, some of these charges may be trapped, thereby reducing the internal electric field experienced by the carriers. If the detrapping lifetime is long, the field can slowly decrease. This reduces the drift velocity of the carriers, which in turn causes more carriers to be trapped.[vi]

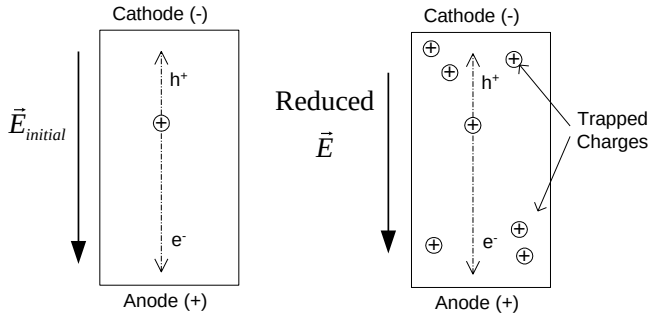

Figure 12. Sketch illustrating polarization in CdTe diodes.

Figure 13 and Figure 14 show a series of CdTe spectra taken over time. Figure 13 shows data taken at room temperature and a low bias voltage, 200V over the 0.75 mm, demonstrating polarization. After only two hours there is a visible change to the spectrum. The effect is the same as reducing the bias voltage: the tailing increases, therefore the peak shifts to lower amplitude, more counts are in the tail, and the peak height degrades. This is clear after only a few hours. Figure 14 shows similar data but with the detector at 220 K and 750V bias, and showing data taken over a 96 hour interval. The stability of the spectra and the absence of polarization are quite clear. These are the normal operating conditions for the XR100T-CdTe.

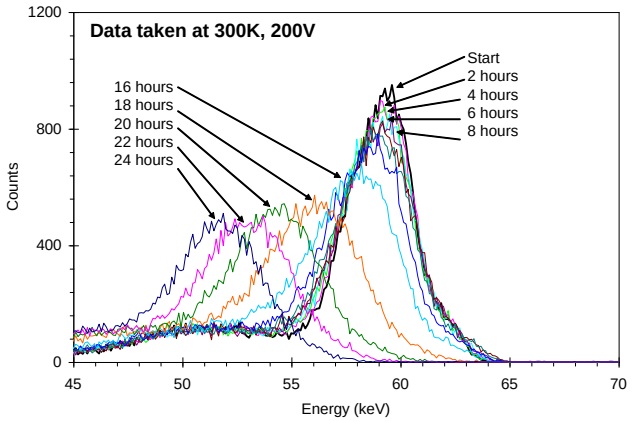

Figure 13. Plot showing spectra taken with a 0.75 mm CdTe detector at room temperature and low bias voltage, over a 24 hour interval, demonstrating polarization.

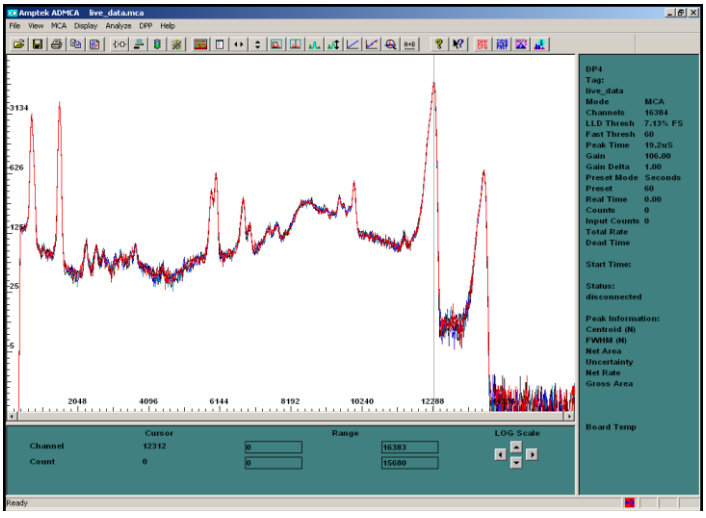

Figure 14. Plot showing spectra taken with a 0.75 mm CdTe detector at 220 K and 750V bias over a period of 96 hours, showing that polarization is not important under the operating conditions of the XR100-CdTe.

3.2.1 Reproducibility

The charge collection properties of CdTe depend on the defect density, which can vary quite strongly if the crystal growth process is changed or even along a single boule, so it is important to consider how much difference one can expect from one detector to the next. Figure 15 shows ^{241}Am spectra measured by twenty detectors in a typical production lot. One detector has a noticeable different spectrum, with both higher electronic noise and worse tailing, but the other 19 have a nearly identical response.

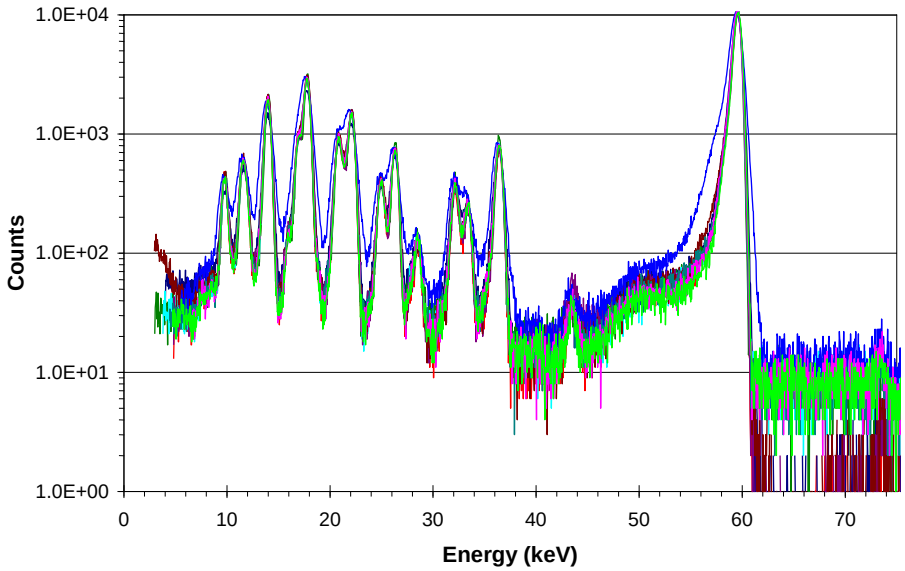

Figure 15. ^{241}Am spectra measured by twenty CdTe detectors in a typical production lot.

4 GENERAL PROPERTIES OF HOLE TAILING

There are some very important conclusions we can make regarding general properties of hole tailing.

1) Hole tailing will be important in any application in which the distance the carriers travel is on the order of or larger than the trapping length ($\lambda=\mu\tau\mathcal{E}$) for either carrier. In such cases, one will always observe an asymmetric photopeak, with a tail towards lower amplitudes. Note that the distance the carriers travel is determined both by the physical size of the detector and on the attenuation depth.

2) The detailed shaping of the tail and the importance of hole tailing depend strongly upon the energy of the photons one is measuring. Low energy photons will always stop near the front contact and will therefore always experience complete charge collection. Hole tailing will be negligible for sufficiently low energies. Sufficiently high energy photons, with an attenuation length long relative to the detector thickness, are stopped uniformly and thus present the worst hole tailing.

3) The detailed shape of the tail will depend upon the carrier lifetimes, which are not well controlled in wide bandgap semiconductors. Two different detectors, cut from the same boule, can have significantly different hole lifetimes and hence very different tailing profiles for identical operating conditions. Each detector must be individually calibrated and/or selected.

4) It has been observed that there is often a relation between hole lifetime and leakage current: detectors with the shortest hole lifetimes have the lowest leakage currents, and therefore the lowest electronic noise. Such detectors are well suited for low energy measurements, where hole tailing is unimportant and resolution is dominated by electronic noise. Detectors with long hole lifetime and larger leakage currents are better suited for high energy measurements, where resolution is dominated by hole tailing and electronic noise is unimportant.

It is important to note that there does not exist a universally accepted method for including the effects of hole tailing in describing the performance of wide bandgap semiconductors. Different manufacturers quantify performance differently. Some present only the FWHM of the peak at some energy, which mixes electronic

noise and hole tailing. Some present only the upper half-width at half maximum, and some refer to twice this as the "FWHM". This is only electronic noise so does not at all address hole tailing.

5 SOLUTIONS

Given that charge transport is a major problem in CZT, and in other wide bandgap semiconductors, four primary solutions have been used to improve spectroscopic performance.

5.1 CRYSTAL GROWTH

The ideal solution would be to learn how to grow crystals without defects. A great deal of research has gone into this, and is still going into this, and significant improvements have been made. The hole $\mu\tau$ in CZT haS increased several-fold over the past few years and will probably continue to improve. Each boule now contains larger single crystals, and the spatial variations in material have decreased. Continued improvements are likely, but it seems extremely unlikely that CZT will approach the characteristics of Si and Ge any time soon. It is inherently more difficult to grow a defect-free compound semiconductor, with two or more constituents, than one made from a single element. In the compound semiconductor, each atom in the lattice must be in the correct place. A slight excess of the atoms of one element at the lattice location where the crystal is growing will lead to defects. So while trapping lengths and uniformity will improve, allowing growth of large crystals, hole tailing is likely to be important for quite a while. A variety of other solutions have therefore been explored.

5.2 COOLING AND M-π-N STRUCTURES

One obvious means of improving charge collection is to apply a higher electric field, but this results in increased leakage currents and therefore increased electronic noise. What this means is that the optimum bias voltage depends upon the details of a user's application. For the detection of X-rays, which stop near the front contact and for which hole tailing is unimportant, a reduced bias voltage will often improve performance by reducing electronic noise. For the detection of γ-rays, if one requires high efficiency and does not need the ultimate in resolution, then an increased bias voltage will help.

Cooling the crystal will reduce the leakage currents, permitting a higher bias voltage with no loss of resolution. For CZT, which has a fairly low leakage current at room temperature, only slight cooling provides significant improvements. A single stage thermoelectric cooler can generate a temperature differential of 50°C, reducing the leakage current by a factor of approximately 100. Alternately, the bias voltage can be increased greatly with little impact on noise. Thermoelectric cooling has major advantages over the cryogenic cooling required for Si and Ge. The cooling is fast (tens of seconds) and, from the user's perspective, all that must be done is to apply power. Thermoelectric cooling is invisible to the user, so the system still operates as if it were at room temperature. Amptek's XR-100T-CdTe systems operate using thermoelectric cooling[vii].

Most CZT detectors are based on the M-S-M structure, in which symmetric metal contacts are placed on a wafer of the semiconductor. The resulting device is symmetric, with no forward or reverse direction. It is also essentially ohmic: the device is fully depleted at a low bias voltage, and for all bias voltages above this the dark current increases linearly with voltage. For many years, research has been carried out into methods of fabricating a diode structure with CZT. With a reverse bias diode the leakage current can be reduced, permitting a higher bias to be applied. Various diode structures have been used, including blocking contacts (M-π-n), doping (P-I-N), and heterojunctions[viii]. Recent research has results in practical methods for fabricating stable M-π-n diodes[ix]. These are used in Amptek's CdTe detectors.

5.3 BIPARAMETRIC METHODS

As should be clear from the previous discussion, the charge collection efficiency of a CZT detector depends upon the depth of the point of interaction. Because of the difference in carrier mobility, the risetime of the preamplifier signal also depends upon the depth of interaction: in interactions close to the front contact, most of the signal is due to the electrons, which travel quickly across the detector. Since both risetime and charge collection efficiency are correlated with depth of interaction, the risetime is therefore correlated with depth of interaction. One can use measurements of the risetime to deduce charge collection efficiency and thus improve spectroscopic performance. Methods based on measuring both risetime and induced charge are termed biparametric methods. Figure 16 shows a measured biparametric spectrum from

a 2x2x2 mm^3 CdTe detector, showing counts versus pulse height and risetime of the shaped output[x]. The maximum pulse heights are observed at the shortest risetimes and are most probable. With increasing risetime, the pulse height decreases and the probability decreases. This is seen very clearly as the channel associated with the 662 keV peak curves towards lower values.

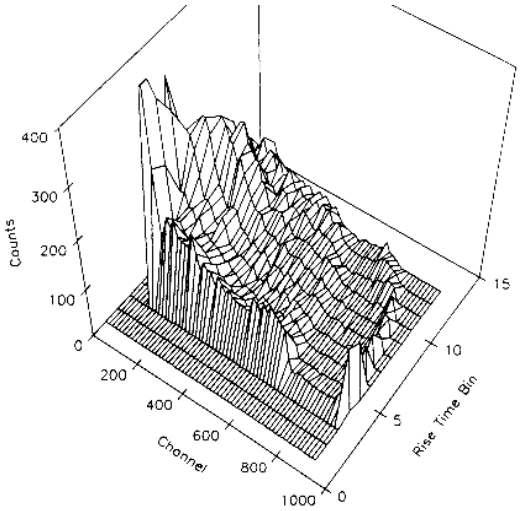

Figure 16. Plot showing the measured distribution of counts versus induced charge and risetime for a ^{137}Cs source, measured with a 2x2x2 mm^3 CdTe detector.

Risetime discrimination (RTD) is one method which has long been used to improve spectral shape using risetime information[xi]. In this method, all pulses with a risetime exceeding some threshold are rejected, thus all pulses that would contribute to the tail are rejected. Amptek offers RTD with XR-100T-CdTe detectors to provide very high resolution. This technique is effective at improving the resolution but leads to significantly reduced sensitivity since many counts are rejected. As can be seen in Figure 4 above, only the top 25% or so of the detector has nearly uniform charge collection. RTD applied to this detector would lead to an effective depth of only 0.5 mm, since the counts in the rest of the volume are rejected.

Some trade-off between resolution and sensitivity is possible: opening the risetime window accepts more counts but these are located in the tail. This is shown clearly in

Figure 17. It should be noted that RTD does not reduce the photopeak sensitivity: the same number of counts will go into the main photopeak with RTD on and off. What RTD does is to reject those that would appear in the tail, which often interfere with lower energy peaks. The “photopeak” region denoted in this plot is a “standardized” region that has been used to compare the performance of many wide bandgap, high-Z semiconductors[xii].

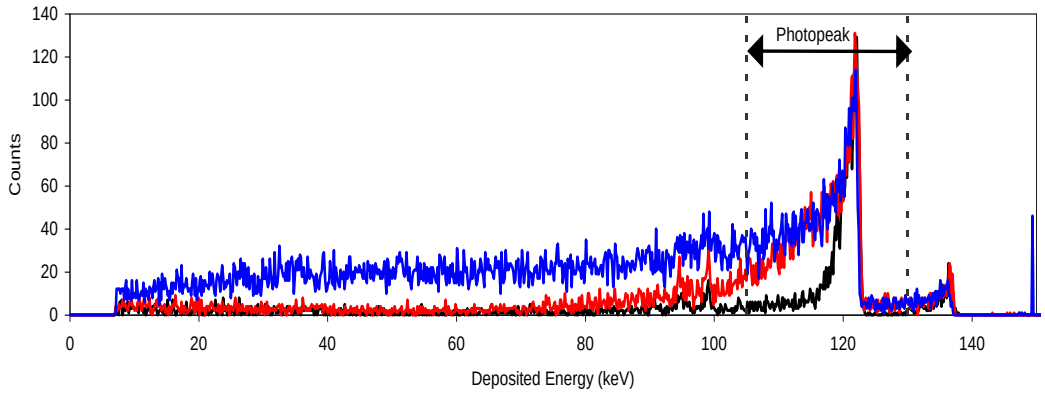

Figure 17. ^{57}Co spectra measured with an XR-100T-CZT with risetime discrimination (RTD) turned off, and turned on at two different settings. All three spectra were taken for the same time, for the same source geometry. The effect of RTD on resolution, total counting efficiency, and photopeak efficiency are clear.

Risetime compensation is an alternate biparametric method in which both the induced charge and the risetime are measured and then, from the risetime, the charge collection efficiency is deduced. The measured induced charge is multiplied by an appropriate correction factor, yielding a corrected pulse amplitude[xiii]. This is a very powerful technique, permitting very high resolution with no loss of sensitive volume. However, there are certain disadvantages. First, the electronics required to measure the risetime and apply any compensation are rather complicated. Second, as can be seen in Figure 16, the pulse height deficit depends non-linearly on risetime. Some commercial devices apply a linear correction, but this is obviously valid only over a limited depth of the detector. Research systems have been developed to apply non-linear corrections which used the entire depth of the detector, but because of their complexity and the difficulty of doing a non-linear calibration on each detector, these systems have not made it into commercial use.

Biparametric techniques have a fundamental limitation in that they are only applicable to pure photoelectric interactions. If an incident photon undergoes a photoelectric interaction, it deposits all its energy at a single point, for which there are two well-defined parameters, risetime and charge loss. If a photo undergoes first a Compton scatter and then photoelectric absorption, then energy is deposited at two depths in the crystal and there are four parameters, a risetime and a charge loss for each interaction point. The deduced charge loss does not precisely equal the charge loss for either depth or the mean charge loss, so some loss of resolution results. For 662 keV photons interacting in a 2 mm CZT detector, the number of photons undergoing a pure photoelectric interaction is comparable to the number first undergoing a Compton scatter and then a photoelectric absorption.

5.4 SINGLE CARRIER COLLECTION

It was noted before that the electrons are almost fully collected for interactions occurring throughout the detector volume and that hole tailing is due only to the signal from holes. If one could measure the current due only to the electrons, and neglect that due to the holes, then the measured charge would not depend on depth. This was done long ago for ion chambers, by locating a grid between the anode and cathode. Only the current due to electron drift between the grid and the anode is measured, resulting in a signal due only to electrons. It is quite difficult to fabricate a grid inside a semiconductor detector. In recent years, a variety of techniques have been developed in which the contacts on the surface of the detector are patterned and read out in such a way that the output signal is due only to electrons. These techniques include hemispherical detectors[xiv], coplanar anodes[xv], small pixel detectors, a geometrically weighted grid[xvi], and a variety of others. The development of detectors using these contacts is a very active and promising field of research, for large volume CZT detectors used in γ-ray detection.

Amptek previously used $Cd_{1-x}Zn_xTe$ (CZT) as the detector material but is now using CdTe diodes. The new detectors differ in three major ways: (1) the basic material is different (CdTe vs. CZT), (2) the CdTe devices are fabricated using blocking (Schottky) diodes rather than the symmetric contacts on CZT, and (3) the standard thickness has been reduced to 1 or even 0.75 mm. The CdTe-Stack detectors utilize several thin (0.75 mm) planar elements to achieve a thickness of 2.25 or 3.75 mm[xvii]. As described in this note, CdTe has superior charge transport properties, so a much improved spectrum is observed. The diode structure permits a higher electric field to be applied, at a comparable leakage current level, further improving charge transport. The use of thin planar elements further improves charge transport, greatly reducing spectral distortions due to hole tailing and ensuring that the entire volume contributes to the photopeak.

6 REFERENCES

[i] For more information on the general properties of radiation detection, refer to Knoll or Tsoulfanidas, which are standard textbooks on radiation detection and measurement.

[ii] For more information on compound semiconductors in radiation detection, refer to the conference proceeding, **Semiconductors for Room Temperature Nuclear Detector Applications**, ed. T.E. Schlesinger and R.B. James, Academic press, 1995

[iii] M.R. Squillante, K.S. Shah, *Other Materials: Status and Prospects*, p 465 in **Semiconductors for Room Temperature Nuclear Detector Applications**, ed. T.E. Schlesinger and R.B. James, Academic press, 1995

[iv] S.M. Sze, **Physics of Semiconductor Devices**, Wiley & Sons, 1981

[v] J.W. Mayer, *Search for semiconductor materials for gamma ray spectroscopy*, p 445 in **Semiconductor Detectors**, ed. G. Bertolini, A. Coche, Wiley (1968)

[vi] H.Toyama, A. Higa, M. Yamazato, et. al., *Quantitative analysis of polarization phenomena in CdTe radiation detectors*, Japanese Jour. Appl. Phys, Vol 45, No 11, 2006

[vii] Pantazis, J.A., A.C. Huber, P. Okun, M.R. Squillante, P. Waer, G. Entine, *New, High Performance Nuclear Spectroscopy System Using Si- PIN Diodes and CdTe Detectors*, IEEE Trans. on Nuc. Sci., Vol. 41, No. 4, (1994)

[viii] M.R. Squillante, G. Entine, E. Frederick, L. Cirignano, T. Hazelett, *Development of two new M-π-n CdTe sensors*, Nucl. Instrum. Meth. A 283 (1989) p 323

[ix] T. Takahashi, B. Paul, K. Hirose, C. Matsumoto, R. Ohno, et al, *High-resolution Schottky CdTe diode for hard X-ray and gamma-ray astronomy*, Nucl. Instrum. Meth. A436 (1999), p 111.

G. Sato, T. Takahashi, M. Sugiho, M. Kouda, *Characterization of CdTe/CdZnTe detectors*, IEEE Trans. Nucl. Sci. Vol 49 No 3, June 2002, p 1258.

[x] R. Redus, M. Squillante, J. Lund, *Electronics for high resolution spectroscopy with compound semiconductors*, Nucl. Instrum. Meth. A 380 (1996) p 312

[xi] Jones & Woollam 1975 (in Eisen 1994), Hagemann 1988, Arlt 1992

[xii] M. Squillante, L. Cirignano, R. Grazioso, *Room-temperature semiconductor device and array configurations*, Nucl. Instrum. Meth A458 (2001) pp 288-296.

[xiii] M. Richter, P. Siffert, *High resolution gamma ray spectroscopy with CdTe detector systems*, Nucl. Instrum. Meth A322 (1992) p 529

R. Redus, M. Squillante, J. Lund, *Electronics for high resolution spectroscopy with compound semiconductors*, Nucl. Instrum. Meth. A380 (1996) p 312

[xiv] M. Richter, P. Siffert, *High resolution gamma ray spectroscopy with CdTe detector systems*, Nucl. Instrum. Meth. A322 (1992), p 529

[xv] P.N. Luke, M. Amman, J.S. Lee, B.A. Ludewigt, H. Yaver, *A CdZnTe coplanar-grid array for environmental remediation*, Nucl. Instrum. Meth. A 458 (2001) p 319

[xvi] D.S. McGregor, R.A. Rojeski, A. He, D.K. Wehe, M. Driver, M. Blakely, *Geometrically weighted semiconductor Frisch grid radiation spectrometers*, Nucl. Instrum. Meth. (1998)

[xvii] R. Redus, A. Huber, J. Pantazis, T. Pantazis, T. Takahashi, S. Woolf, *Multielement CdTe stack detectors for gamma-ray spectroscopy*, IEEE Trans. Nucl. Sci. 51 (5) , 2004 (p 2386)